Chapter 9
Instrumental Data on the Seismic Activity Along the Dead Sea Transform

Abraham Hofstetter, Catherine Dorbath, and Louis Dorbath

Abstract We analyzed the catalog of instrumental recordings of seismic activity from 1900 to 2010 along the Dead Sea Transform. The seismicity pattern reveals significant activity confined to 5 main sections of the transform. In all the sections of the transform there is a significant amount of seismic activity at depths of 9–10 km (lower part of the upper crust). The seismic activity extends to large depths of 20 km and more, where about 30 % of the seismic activity occurs in the lower crust, especially in the Dead Sea basin and the Arava Valley. The deep seismicity is correlative with previous low heat flow measurements along the transform, and thus suggesting a relatively cold crust. We analyzed more than 4,300 S-wave spectra of earthquakes in the magnitude range is $0.8 \leq M_d \leq 6.2$, with M_0 values ranging from $3.1 x 10^{11}$ N·m to $5.4 x 10^{18}$ N·m, and Brune stress drop estimates, $\mathbf{\Delta}\sigma$, between 0.1 MPa and 15 MPa. The total seismic moment release in the years 1900–2010 in the Dead Sea Transform due to all the earthquakes, including the earthquake in 1927, is only a fraction of the expected seismic moment release.

A. Hofstetter (✉)
Geophysical Institute of Israel, Lod 71100, Israel

Ecole et Observatoire des Sciences de la Terre,
University of Strasbourg, Strasbourg 67000, France
e-mail: ramih@gii.co.il

C. Dorbath
Ecole et Observatoire des Sciences de la Terre, University of Strasbourg,
Esplanade, Strasbourg 67000, France

IRD, UMR 154, 14 Avenue Edouard Belin, Toulouse 31400, France
e-mail: c.dorbath@unistra.fr

L. Dorbath
Ecole et Observatoire des Sciences de la Terre, University of Strasbourg,
Strasbourg 67000, France
e-mail: louis.dorbath@eost.u-strasbg.fr

9.1   Introduction

The Dead Sea Transform (DST), which accommodates the left-lateral motion between the Sinai Subplate and the Arabian plate, is about 1,200 km long, connecting the Taurus-Zagros compressional front, in the north, to the extensional zone of the Red Sea, in the south. Over the past few million years tectonics has shaped the Dead Sea Transfrom (e.g., Freund et al. 1970; Ben-Menahem et al. 1976; Ben-Avraham et al. 2008). The Dead Sea Transform comprises a few major basins being connected by several large faults, where the Dead Sea basin is the largest one.

Based on historical accounts and instrumental records, some describing harmful or devastating earthquakes, it is clear that the Dead Sea Transform poses a major seismic threat to the population on both its sides. Figure 9.1 illustrates the locations of all instrumentally recorded earthquakes occurring between 1900 and 2010 along the Dead Sea Transform, or in the commencement of its branching-out faults or nearby faultings, a total of about 3,800 earthquakes. The seismic activity is somewhat spread in the transform with no clear lineation and thus we include seismic activity up to about 10 km on both sides of the transform. We also inserted improved locations of epicenters in the Dead Sea basin (after Hofstetter et al. 2012), based on the tomoDD algorithm of Zhang and Thurber (2003). One notable earthquake is the July 11, 1927 earthquake, M 6.2, which occurred in the northern part of the Dead Sea basin resulting in 285 deaths, 940 wounded, and extensive damage in many towns and villages on both sides of the Dead Sea Transform (Ben-Menahem et al. 1976; Shapira et al. 1992; Avni 1998). Throughout the twentieth century, several other widely felt earthquakes occurred in 1903, 1928, 1956, 1970, 1979 and 2004, with magnitudes M ~5.0–5.5, causing no or minor damage (e.g. Arieh et al. 1982; Amiran et al. 1994). However, five out of seven relatively moderate-strong events occurred in the Dead Sea basin and two occurred just north of the basin.

In the past decades a series of intensive seismological studies improved our understanding of the seismotectonic activity of the Dead Sea Transform, i.e., Ben-Menaham et al. (1976) and Salamon et al. (1996, 2003) studied the seismicity along the Sinai sub-plate. Arie et al. (1982), Shapira and Feldman (1987), Van Eck and Hofstetter (1989, 1990), Shapira (1997) and Hofstetter et al. (2007) studied the seismic activity in the Dead Sea basin and along the Dead Sea Transform exhibiting complex focal mechanisms. Rotstein et al. (1991) and Shamir et al. (2006) studied the structure of the northern Dead Sea basin and the Jericho valley based on a series of earthquakes including the mainshock in 2004. Salamon (2005), Al-Tarazi et al. (2006) and Hofstetter et al. (2008) described the effects of the mainshock in 2004 and their tectonic implications. Below we focus our attention on instrumental data obtained from the seismic activity along the Dead Sea Transform, which is listed in the catalog from 1900 to 2010 (http://www.gii.co.il/home.html), where the latitude range is from 29.5°N (northern tip of the Gulf of Aqaba) to 33.5°N (southern
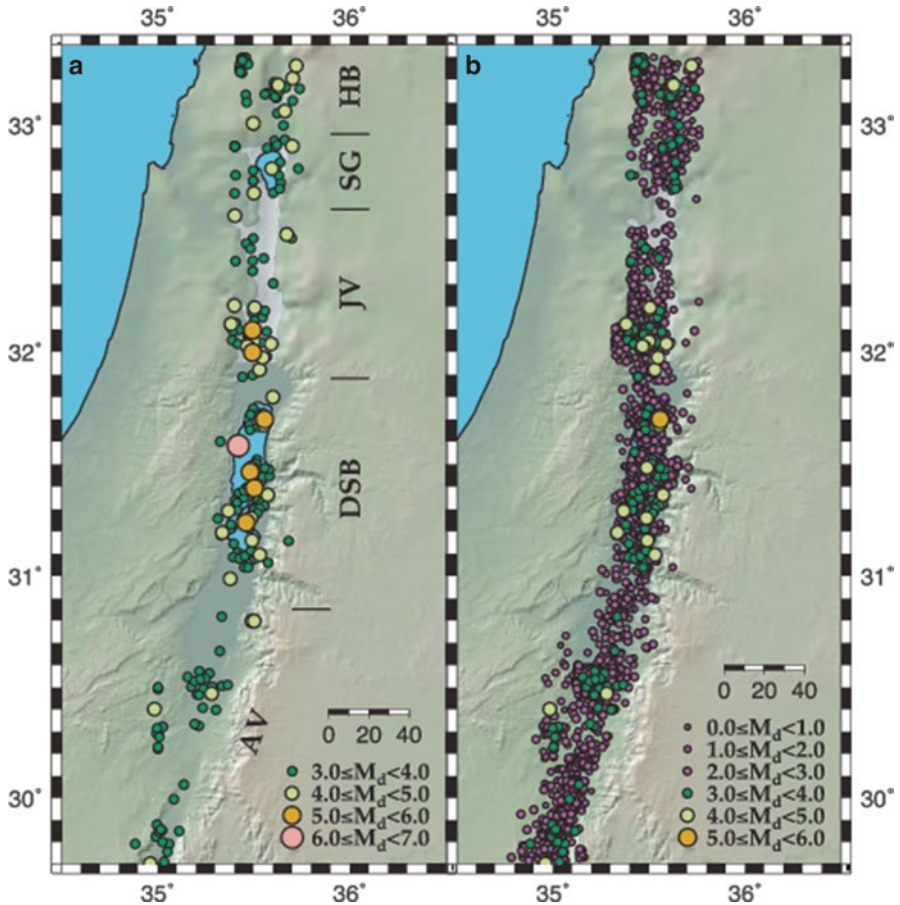
Fig. 9.1 Earthquakes that occurred along the Dead Sea Transform in the time periods: (**a**) 1900–2010, $M_d \geq 3$; (**b**) 1983–2010, all magnitudes. The Dead Sea Transform is divided to five main sections: *AV* Arava Valley, *DSB* Dead Sea basin, *JV* Jordan valley, *SG* Sea of Galilee, *HB* Hula Basin

Lebanon), as was recorded by the short period and broad band stations of Jordan and Israel, and using the coda magnitude (Shapira 1988).

9.2   Data and Acquisition Systems

The seismic monitoring in the Middle East started in the end of the nineteenth century with the installation of station Helwan (HLW) in Cairo, Egypt. From 1898 until 1912 Helwan was the only seismological station that operated in the region, along with some other more remote operating stations like Athens and Istanbul. Another important station that started operating in 1912 was Ksara, which is located in central-east part of Lebanon. Station JER of the WWSSN, located in the Hebrew University of

Jerusalem, started operating in 1954, and was later upgraded in 1963. During the middle of the twentieth century temporary stations operated for a short period of time in various part of Israel enriching somewhat the seismological catalog. Two relatively large seismic networks, with up to 35 short period stations in each network, have been installed in 1983, one in Jordan (JSO, Jordan Seismological Observatory) and the other in Israel (ISN, Israel Seismic Network), reaching stabilization within a year. With time those networks have been upgraded and several broad band stations and many accelerometers have been installed. Since that time the seismicity of the Dead Sea Transform is continuously monitored by the ISN and JSO (Fig. 9.2). In 2000 the catalogs of both networks were merged to create a common Dead Sea Transform catalog, and it is an ongoing process since then.

In addition to the above mentioned permanent networks, a few temporary networks, each time for about 1–2 years, were operating in the Dead Sea Transform or near its outskirts significantly enriching the database. The temporary network added important information, however, still the main backbone of the catalog is based on the permanent networks. Those campaigns include: (1) a portable network comprising of 6 stations that operated in the Dead Sea basin in 1983–1984 and later north of Eilat in 1984–1985; (2) a 12-station-network around the Dead Sea basin in 1986–1988; (3) a large network including up to 70 stations in Jordan and Israel south of the Dead Sea Lake, known as DESERT2000 (i.e., Weber et al. 2004), and crossing the Dead Sea Transform in the Arava Valley in a WNW-ESE line operating from April 2000 to May 2001; (4) a more condensed network in the Dead Sea basin and its immediate outskirts comprising up to 70 stations and operating from Oct. 2006 to May 2008, known as DESIRE (i.e., Weber et al. 2009a, b; Braeuer et al. 2012a, b). The seismicity presented here is based on the compilation of data, collected by all the above-mentioned networks.

9.3   Distribution of Seismicity in Space and Time

Figure 9.3a, b presents the distribution of earthquakes along the Dead Sea Transform as a function of depth and time and also the accumulated number of earthquakes as a function of depth. We avoid all depth determinations prior to 1981, which were usually obtained using a small number of stations or seismic phases. Epicentral location errors are about ±2–3 km for most of the events and about ±3–5 km for the depth. Location errors are significantly smaller in the case of events that were reported by DESIRE, or once we apply local earthquake tomography (Hofstetter et al. 2012; Braeuer et al. 2012a, b) for the events in the Dead Sea basin and its adjacent regions. The number of earthquakes in this time period is relatively small (see Fig. 9.3c) so it does not cause any major bias of the observations. We mark the limits of the five main sections of the DST: Arava (AV), Dead Sea basin (DSB), Jordan Valley (JV) north of the Dead Sea Basin and south of the Sea of Galilee Basin (SG) and Hula Basin (HB). The horizontal dashed lines (Fig. 9.3b) mark the inner schematic division of the crust into the upper and lower parts and the uppermost part of the mantle, essentially an average of several studies that were conducted along or across the Dead Sea Transform (Ginzburg et al. 1979a, b; El-Isa et al. 1987; ten
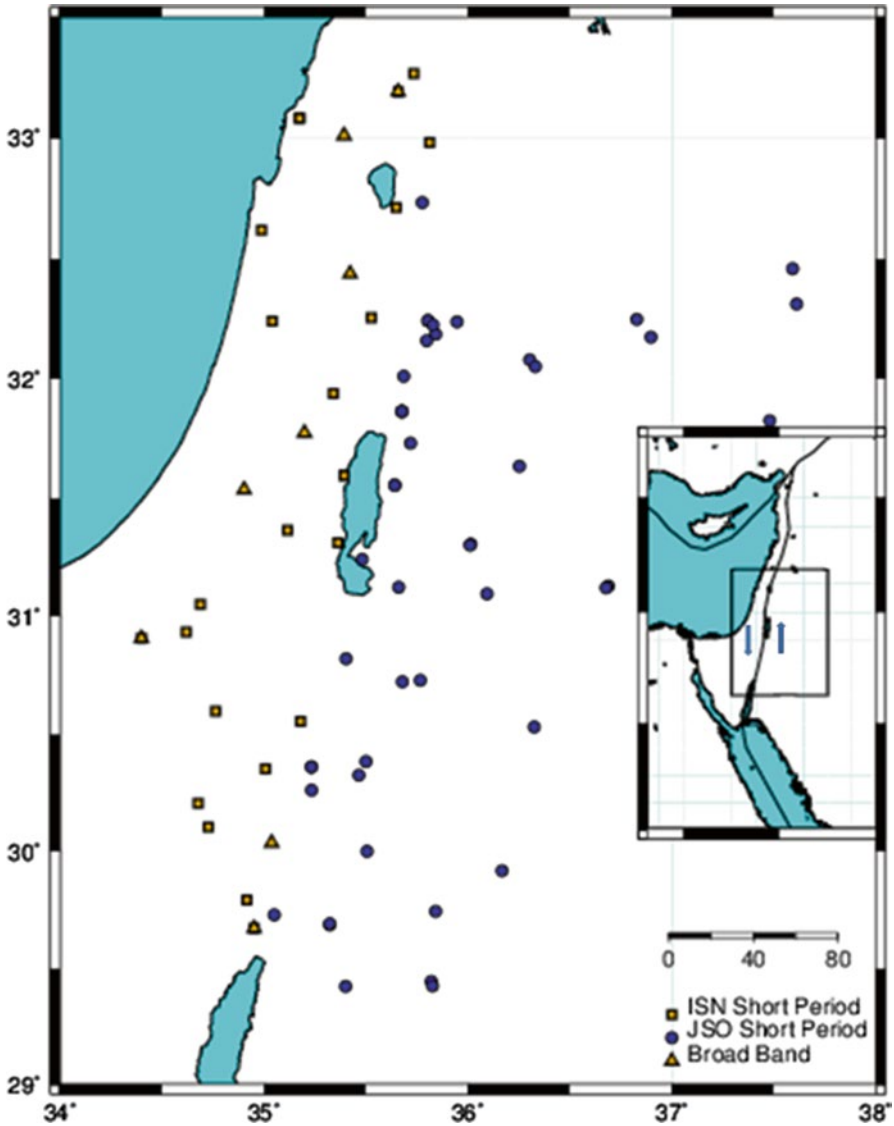
Fig. 9.2 Location of short-period seismic stations (*square*) and broadband stations (*triangle*) that were used for the location of earthquakes along the Dead Sea Transform. The proximity of some stations is due to the fact that the sites of some stations were changed due to technical issues during this period of time. The inset represents a schematic Middle East tectonics where the rectangle marks the study area of the Dead Sea Transform, and the blue arrows present the principal plate movement on both sides of the transform

Brink et al. 1993, 2006; Gitterman et al. 2006; Mechie et al. 2009). Most of the seismic activity, in the Sea of Galilee and Jordan Valley, occurs in the upper crust with two peaks at depths of 2–3 km and about 9–10 km (Fig. 9.3b). The activity in the HB is relatively constant at all depths. Most of the seismic activity in the Dead
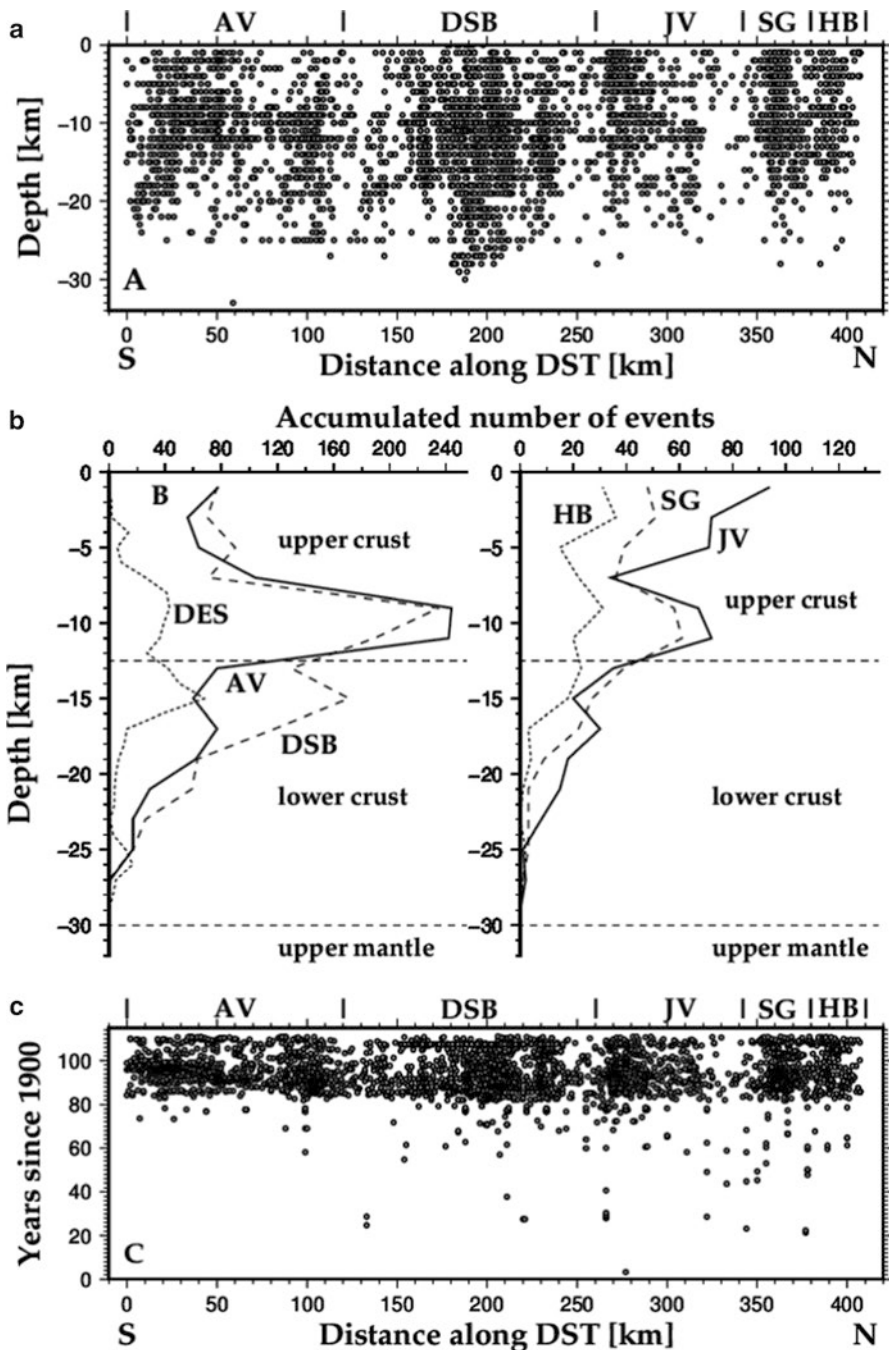
Fig. 9.3 (**a**) Distribution of earthquakes as a function of depth along the Dead Sea Transform based on recordings of permanent and temporary stations, where *AV* Arava Valley, *DSB* Dead Sea basin, *JV* Jordan valley, *SG* Sea of Galilee, *HB* Hula Basin (*lower part*); (**b**) Accumulated number of events as a function of depth in the crust and upper part of the upper mantle (*upper part*) in the five sections of the DST, where AV (solid line) DSB (*dashed line*) on the left side and JV (*solid line*), SG (*dashed line*) and HB (*dotted line*) are on the right side. The *horizontal dashed lines* present

Sea basin and Arava fault is deep with a pronounced peak at about 9–10 km and a secondary peak, in the case of DSB, at a depth of 15–16 km. The seismic activity at shallow depths in DSB and AV is rather minimal as compared to the deeper ones.

In all the sections along the transform there is significant amount of seismic activity in the lower crust, with a clear peak in the DSB at about 15–16 km. Seismic activity extends nonuniformly down to depths of 20 km and more in all sections of the Dead Sea Transform, mainly in AV, DSB, JV and SG. In total, in the Dead Sea Transform 1,220 out of 3,800 earthquakes (about 30 %) have deep hypocenters in the lower crust. Several heat flow studies reported on low values along the DST except for the Sea of Galilee basin (Ben-Avraham et al. 1978; Feinstein 1987). Recently, Förester et al. (2007) reported low values near the SG and AV and higher values in the eastern margin of the transform. The occurrences of hypocenters in the lower crust, as were also reported by Aldersons et al. (2003) and Hofstetter et al. (2012), requires a relatively thick brittle part of the crust. It can be are in a good agreement with the observations of the low heat flow measurements, suggesting relatively cold crust. Förester et al. (2010) and Petrunin et al. (2012) argued that the heat flow should be 50–60 mW m^{-2}, and in the Dead Sea basin the brittle layer is about 20–22 km and up to 27 km locally. The maximal depth of earthquakes throughout the Dead Sea Transform is about 25 km and even deeper in some parts, i.e. the Dead Sea basin (Fig. 9.3). The DESIRE campaign enriched the database of the Dead Sea basin, however, one can expect that comparable results could have been obtained in other parts of the Dead Sea Transform had similar campaigns been operating there.

Most of the seismic activity in the DST occurs in the middle of the sections while in the borders between two adjacent sections it is rather limited. This fact agrees with observations of Hofstetter et al. (2012) regarding the seismic activity at the northern and southern ends of the Dead Sea Basin. Out of seven relatively moderate to strong earthquakes ($M_d \geq 5.0$) that occurred along the DST only two are located in the section of the Jordan Valley, just north of the Dead Sea basin, in 1903 and 1928, and all the other earthquakes in 1927, 1956, 1970, 1979 and 2004 are located in the Dead Sea basin. Furthermore, the epicenters of all those earthquakes are located within the basin and relatively far from the southern or northern basin ends, i.e. the strong earthquake of 1927 with M 6.2.

The distribution of earthquakes along the DST as a function of time is presented in Fig. 9.3c. It is clear that the rate of occurrence from the early 1980s of last century is relatively uniform throughout the whole DST, with some temporal higher rate of activity from time to time. If we use only the observations of the permanent seismic networks of Jordan and Israel then for $M_d \geq 2.0$ the rate of "earthquake productivity" is rather uniform of about 7–9 earthquakes/km/year in the last 30 years in the five sections of the Dead Sea Transform. The fact that until the 1980s the number of reported earthquakes is rather small, can be explained by the sparse operating regional stations in the whole region, which hampers the possibility to identify any significant change in

---

Fig. 9.3   (continued) schematic inner division of the crust and upper mantle (After Ginzburg et al. 1979a, b; El-Isa et al. 1987; ten Brink et al. 1993, 2006; Gitterman et al. 2006; Mechie et al. 2009); (**c**) Distribution of earthquakes as a function of time along the Dead Sea Transform. The DESIRE recordings, marked as DES, are mainly in the Dead Sea basin

the seismic activity at any section of the DST. Furthermore, in those years the Arava Valley appears to be depleted from any seismic activity, as there were no operating local stations in its vicinity recording the microearthquake activity. Any strong earthquake that might occur in the Arava Valley would have been recorded by some distant regional stations, which is the case for several moderate to strong earthquakes that occurred in the other sections and were recorded by the sparse regional network in the Middle East.

The DESIRE campaign focused mainly on the southern Dead Sea basin, providing very detailed measurements in this region (Weber et al. 2009a, b; Braeuer et al. Braeuer et al. 2012a, b) during 18 months. The DESIRE recordings were added in Fig. 9.3. Most of the events were of small magnitudes and were not recorded by the permanent networks of either Jordan or Israel. In this study, as observed also by the permanent networks, there is the clear indication of seismic activity essentially at all depths down to about 30 km. The activity as a function of the depth as resulted from the 3-D inversion using the SIMULPS algorithm, done by Braeuer et al. (2012b; Fig. 9.3b therein), are presented also in Fig. 9.3b and marked as DES. There are two clear activity peaks at 9, 15 km and a small peak at 26 km. The shape of the event-depth distribution is similar to the equivalent distribution of DSB. We note that the second peak in the event-depth distribution of DES at 15 km is the largest one as compared to the peak at 9 km (by about 50 %), while in the DSB event-depth distribution we get the opposite order. However, we suppose that a longer period of recording time is needed in order to reach a more conclusive determination of the pattern of the seismic activity.

Catalog completeness was studied by Shapira and Hofstetter (2002; see also http://www.gii.co.il) for the period 1900–2000, taking into account the small number of local and regional seismic stations in the first half of the twentieth century anywhere in the Middle East, and the increasing number of seismic stations in the second half in Israel, Jordan and neighbouring countries. Through this period of time the detectability of seismic events has been improved and catalog completeness is considered in the following time steps: $M_d \geq 5.0$ from 1900 to 1939, $M_d \geq 4.0$ from 1940 to 1962, $M_d \geq 3.0$ from 1963 to 1982, and $M_d \geq 2.0$ from 1983 to recent times. The detectability of earthquakes in the Dead Sea Transform is rather uniform as a consequence of the operation of both seismological networks in Israel and Jordan since 1983, and the fact that there is a large number of operating stations on both sides of the transform.

Shapira and Hofstetter (2002) determined the b-value using a maximum likelihood method (Aki 1965; Wiechert 1980) for the time period 1900 through 2000, a total of 100 years, to be 0.96. There was no significant change in the seismic activity in the last 11 years and our results are very similar to those of Shapira and Hofstetter (2002). Overall there is a good agreement with the b-values obtained in former studies, i.e., by Salamon et al. (1996), b=1.00 for the whole Dead Sea Transform (from southernmost part of Sinai to Eastern Turkey) for a 95 year period. The b-value is within the error bounds (about 0.05 to 0.1 units) of recent studies of Arieh (1967), b=0.8 for a 60 year period, Ben-Menahem and Aboodi (1971), b=0.86 for a 2,500 year period, and Shapira and Feldman (1987), b=0.8 for a 10 month period, although different magnitude scales and regions were used in these studies.
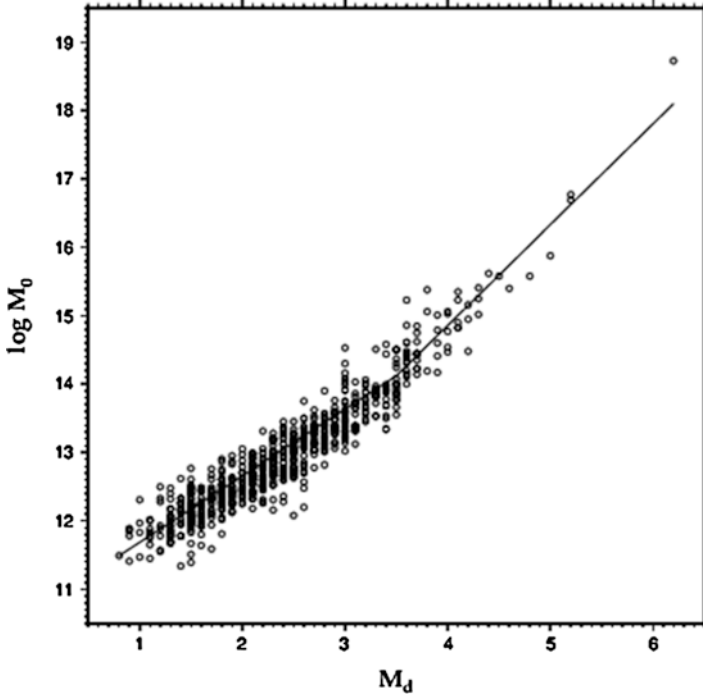
Fig. 9.4 The relation between the seismic moment M_0 and the magnitude M_d, including seismic moment of the earthquake of 1927 (After Ben-Menahem et al. 1976)

9.4   Seismic Moment and Stress Drop Estimation

We calculate the seismic moment, M_0, corner frequency, f_0, stress drop, $\Delta\sigma$, and source radius, r_0 based on the dislocation model of Brune (1970, 1971), using the spectra of S-waves recorded by the short period stations (three-components or vertical component) or the broadband stations in the case of relatively strong earthquakes. Here we describe briefly its application to the Israel Seismic Network following Shapira and Hofstetter (1993).

We manually analyzed more than 4,300 S-wave spectra, with M_0 values ranging from $3.1x10^{11}$ N·m to $5.4x10^{18}$ N·m. We assume the relationship $\log M_0 = aM_d + b$ between the mean seismic moment M_0 and the coda magnitude M_d of a given earthquake. The best fit is simultaneously obtained for two parts of the magnitude range and we get for the first part

$$\log M_0 = (0.9 \pm 0.1)M_d + (10.7 \pm 0.4),\ 0.8 \leq M_d < 3.5$$

and for the second part

$$\log M_0 = (1.5 \pm 0.1)M_d + (8.8 \pm 0.3),\ 3.5 \leq M_d < 6.2$$

where M_0 is in N·m and the magnitude range is $0.8 \leq M_d \leq 6.2$ (see Fig. 9.4). For the small magnitude earthquakes the magnitude coefficients in the first relation are
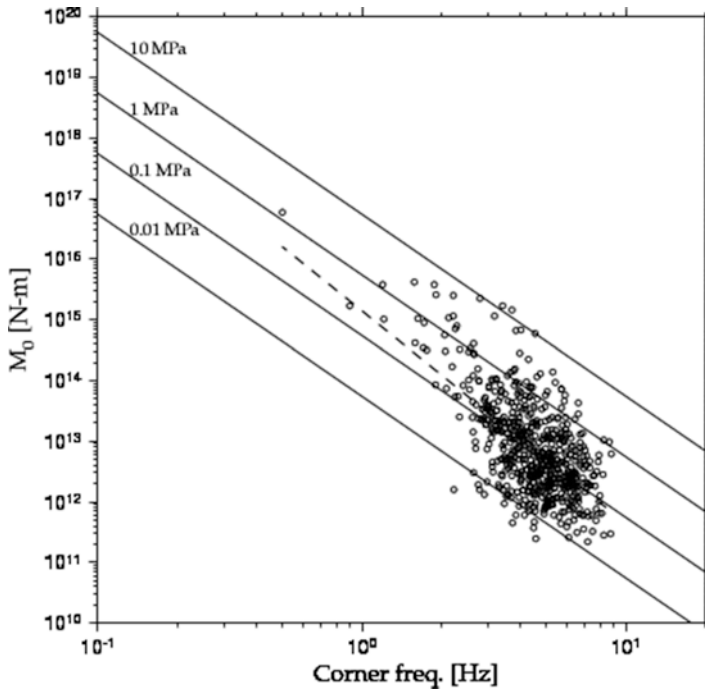
Fig. 9.5 The relation between the corner frequency f_0 and the seismic moment M_0, for the earthquakes in this study, where for reference the solid lines represent stress drop values of 0.01, 0.1, 1 and 10 MPa, based on f^{-3} scaling. The *dashed line* represent a least-squares fit of the observations with a slope of about -3.5

slightly lower than those in similar relations, as obtained by Bakun (1984) and Hanks and Boore (1984) for earthquakes in California, and by van Eck and Hofstetter (1989), Shapira and Hofstetter (1993), Hofstetter et al. (1996), Hofstetter (2003) and Hofstetter et al. (2008) for the Dead Sea Transform, the Carmel fault, the Eastern Mediterranean region, or the Gulf of Aqaba, with relatively similar magnitude range. The second relation is similar to the relation of Hofstetter and Shapira (2000) for earthquakes in the Eastern Mediterranean region.

The corner frequency decreases with increasing seismic moment, as can be seen in Fig. 9.5, where for reference the solid lines represent stress drop values of 1, 10 and 100 bars, based on f^{-3} scaling. We estimate the stress drop of the earthquakes $\Delta\sigma$, based on the dislocation model of Brune (1970, 1971), using the equation $\Delta\sigma = 8.47 M_0 f_0^3 / \beta_s$ where f_0 is the corner frequency, and β_s is the rupture velocity. Shapira and Hofstetter (1993) provided details of the application of the method in the case of seismograms observed by the ISN (short period or broadband). It is similar to former values obtained for earthquakes occurring in the Dead Sea basin (van Eck and Hofstetter 1989) or other parts of the Dead Sea Transform, the Carmel fault and the Gulf of Aqaba (Shapira and Hofstetter 1993; Hofstetter et al. 1996; Hofstetter 2003). In general, the stress drop clearly increases with the increasing seismic
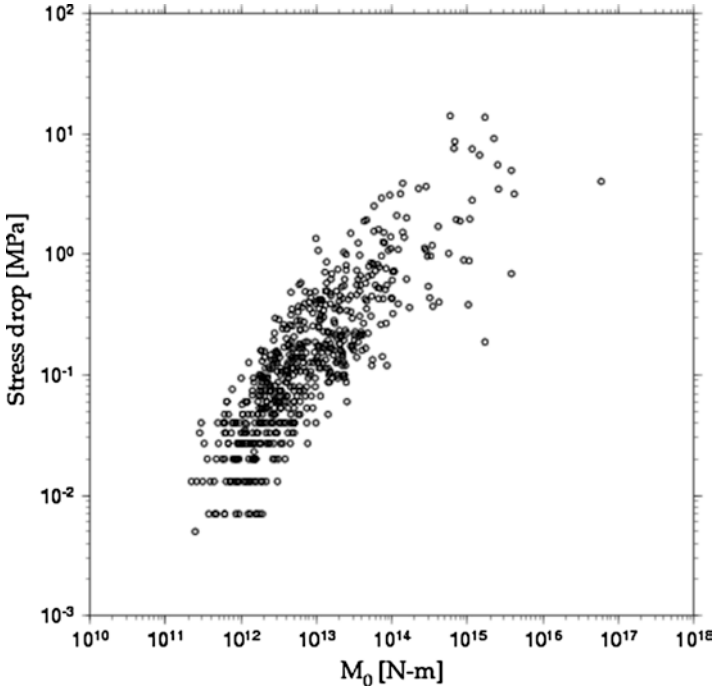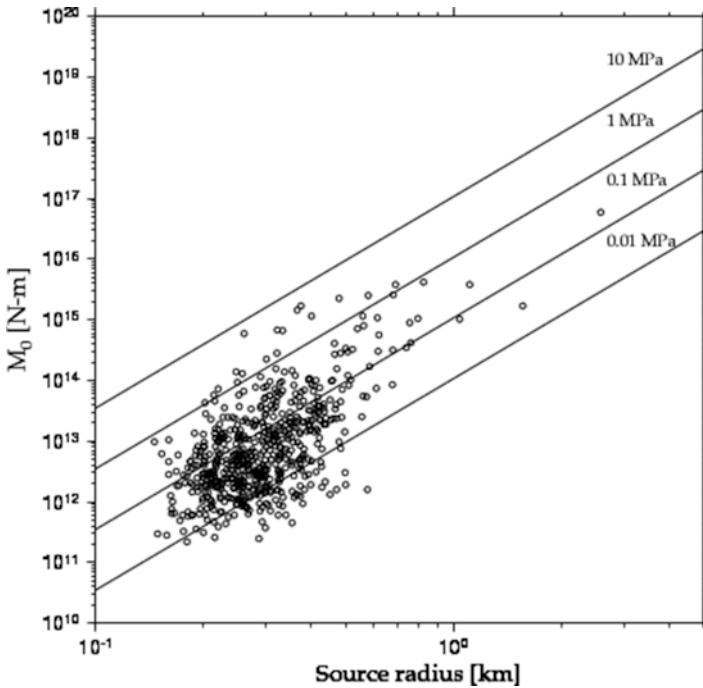
Fig. 9.6 The relation between Brune's stress drop $\Delta\sigma$ and the seismic moment M_0, for the earthquakes in this study

moment (Fig. 9.6), but there is no simple relationship between the stress drop and the seismic moment (or magnitude). This has already been noted for earthquakes in California by Hanks and Thatcher (1972), Thatcher and Hanks (1973), Kanamori and Anderson (1975), and for the Eastern Mediterranean region by Shapira and Hofstetter (1993). Using Brune's model (1970) we estimate the source radius using the relation $r_0 = a(\beta_s/f_0)$ where a has the value 0.37 (Fig. 9.7). Typical source radius values are between 0.2 and 0.6 km for the small magnitude earthquakes.

9.5   Discussion and Conclusions

Figure 9.5 illustrates the relationship between the corner frequency f_0 and the seismic moment M_0, for the Dead Sea Transform. As can be seen our observations suggest a relationship of $\sim f^{-3.5}$. Van Eck and Hofstetter (1989) reported also a steeper fall than -3. It was interpreted by them as f_{max} for frequencies just below 10 Hz. In this case we observe the tendency already at frequencies of 3–4 Hz, which clearly suggests f_0. Mayeda et al. (2007) presented a similar relationship between the seismic moment and corner frequency for the Hector Mine sequence, California, where the scaling of seismic moment and corner frequency does not follow f^{-3} and is consistent with f^{-4}.

Fig. 9.7 The relation between the area *r* and the seismic moment M_0, for the earthquakes in this study, where for reference the *solid lines* represent stress drop values of 0.01, 0.1, 1 and 10 MPa, based on f^{-3} scaling

They used this evidence to support the idea of non-self-similarity, which means that a large earthquake is not a simple integer multiplication of a small one.

When studying the seismic efficiency of the Dead Sea Transform one should take into consideration the total length of the transform (Garfunkel et al. 1981), which is well beyond the section of the transform from the Gulf of Aqaba to Lebanon, shown in this study. The DST is essentially depleted from strong earthquakes except the one in 1927 with the seismic moment of 5.4×10^{18} N m (Ben-Menahem et al. 1976). The seismic moment contribution of the aftershocks of the 1995 sequence (Hofstetter 2003), the moderate activity in 2004 in the northern part of the Dead Sea basin (Hofstetter et al. 2008) and the recent activity in southern Lebanon in 2008–2010 (Meirova and Hofstetter 2012) is relatively minor. Even if we sum up the calculated seismic moment for all the earthquakes in the catalog, based on the above mentioned Mo-Md relationship, including the moderate earthquakes in the Dead Sea basin in 1956, 1970 and 1979, and 2 earthquakes in the Jordan Valley in 1903 and 1928, we still get a small contribution relative to that of the earthquake in 1927, where the latter contributes about 5 % to the total seismic moment, in good agreement with Garfunkel et al. (1981). Salamon et al. (2003) showed that the contribution of the Gulf of Aqaba earthquake in 1995 to the accumulated seismic moment is less than 40 % of the expected sum. They used a rate of relative motion of 5 mm/year.

Recent studies (Wdowinski et al. 2004; Le Beon et al. 2008; Sadeh et al. 2012) reported somewhat smaller slip rate values from 3.1 to 5.4 in various parts of the Dead Sea Transform, and a probable representative average value is 4.3 mm/year. If we use the latter value of slip rate and taking into account the contribution of the 1927 earthquake then the accumulated seismic moment is about 60 % of the expected sum, which means that the transformal motion along the Arabian-Sinai plate border is of major nature. Yet the large difference between the calculated seismic moment and expected moment due to the displacement along the transform is an open question that should be further explored.

The DESIRE campaign provided very detailed measurements in the southern Dead Sea basin and adjacent regions (Weber et al. 2009a, b; Braeuer et al. 2012a, b), which were taken in a period of 18 months. The accumulated seismic moment of these observations is equivalent to an earthquake of Md 4.2, essentially a small contribution. Similar campaigns, for longer periods of time using a large set of seismic stations, should be conducted in other parts of the Dead Sea Transform to better characterize the seismic activity of each part.

References

Aki K (1965) Maximum likelihood estimate of b in the formula log $N = a - bM$ and its confidence limits. Bull Earthq Res Inst 43:237–239

Aldersons F, Ben-Avraham Z, Hofstetter A, Kissling E, Al-Yazjeen T (2003) Lower-crustal strength under the Dead Sea basin from local earthquake and rheological modeling, Earth Planet. Sci Lett 214:129–142

Al-Tarazi E, Sandvol E, Gomez F (2006) The February 11, 2004 Dead Sea earthquake M_L=5.2 in Jordan and its tectonic implication. Tectonophysics 422:149–158

Amiran D, Arieh E, Turcotte T (1994) Earthquakes in Israel and adjacent areas: macroseismic observations since 100 B.C.E. Isr Explor J 44:76–91

Arieh E (1967) Seismicity of Israel and adjacent areas. Geol Surv Isr Bull 43:1–14

Arieh E, Rotstein Y, Peled U (1982) The Dead Sea earthquake of April 23, 1979. Seismol Soc Am Bull 72:1627–1634

Avni R (1998) The 1927 Jericho Earthquake, comprehensive macroseismic analysis based on contemporary sources. PhD thesis, University of Ben-Gurion, Israel, 211 pp. (in Hebrew with English abstract)

Bakun WH (1984) Seismic moments, local magnitudes, and coda-duration magnitudes for earthquakes in central California. Bull Seismol Soc Am 74:439–458

Ben-Avraham Z, Henel R, Villinger H (1978) Heat flow through the Dead Sea rift. Mar Geol 28:253–269

Ben-Avraham Z, Garfunkel Z, Lazar M (2008) Geology and evolution of the Southern Dead Sea fault with emphasis on subsurface structure. Annu Rev Earth Planet Sci 36:357–387

Ben-Menahem A, Aboodi E (1971) Tectonic patterns in the Red Sea region. J Geophys Res 76:2674–2689

Ben-Menahem A, Nur A, Vered M (1976) Tectonics, seismicity and structure of the Afro-Euroasian junction-the breaking of an incoherent plate. Phys Earth Planet Inter 12:1–50

Braeuer B, Asch G, Hofstetter A, Haberland C, Jaser D, El-Kelani R, Weber M (2012a) Microseimicity distribution in the southern Dead Sea area and its implications on the structure of the basin. Geophys J Int 188:873–878

Braeuer B, Asch G, Hofstetter A, Haberland CH, Jaser D, El-Kelani R, Weber M (2012b) High resolution local earthquake tomography of the southern Dead Sea area. Geophys J Int 191:881–897. doi:10.1111/j.1365-246X.2012.05668.x

Brune J (1970) Tectonic stress and the spectra of seismic shear waves from earthquakes. J Geophys Res 73:4997–5009

Brune J (1971) Correction. J Geophys Res 76:5002

El-Isa Z, Mechie J, Prodehl C, Makris J, Rihm R (1987) A crustal structure study of Jordan derived from seismic refraction data. Tectonophysics 138:235–253

Feinstein S (1987) Constraints on the thermal history of the Dead Sea graben as revealed by coal ranks in deep boreholes. Tectonophysics 141:135–150

Förster A, Förster H-J, Masarweh R, Masri A, Tarawneh K, DESERT Group (2007) The surface heat flow of the Arabian Shield in Jordan. J Asian Earth Sci 30:271–284. doi:10.1016/j.jseaes.2006.09.002

Förster H-J, Förster A, Oberhänsli R, Stromeyer D (2010) Lithospheric composition and thermal structure of the Arabian Shield in Jordan. Tectonophysics 481:29–37

Freund R, Garfunkel Z, Zak I, Goldberg M, Weissbrod T, Derin B (1970) The shear along the Dead Sea Rift. Philos Trans R Soc Lond Ser A 267:107–130

Garfunkel Z, Zak I, Freund R (1981) Active faulting in the Dead Sea rift. Tectonophysics 80:1–26

Ginzburg A, Makris J, Fuchs K, Prodehl C, Kaminski W, Amitai U (1979a) A seismic study of the crust and upper mantle of the Jordan-Dead Sea Rift and their transition toward the Mediterranean Sea. J Geophys Res 84:1569–1582

Ginzburg A, Makris J, Fuchs K, Perathoner B, Prodehl C (1979b) Detailed structure of the crust and upper mantle along the Jordan-Dead Sea Rift. J Geophys Res 84:5605–5612

Gitterman Y, Pinsky V, Amrat A-Q, Jaser D, Mayyas O, Nakanishi K, Hofstetter A (2006) Source features, scaling and location of calibration explosions in Israel and Jordan for CTBT monitoring. Isr J Earth Sci 54:199–217

Hanks TC, Boore DM (1984) Moment-magnitude relations in theory and practice. J Geophys Res 89:6229–6235

Hanks TC, Thatcher W (1972) A graphical representation of seismic source parameters. J Geophys Res 77:4393–4405

Hofstetter A (2003) Seismic observations of the 22/11/1995 Gulf of Aqaba earthquake sequence. Tectonophysics 369:21–36

Hofstetter A, Shapira A (2000) Determination of earthquake energy release in the Eastern Mediterranean region. Geophys J Int 143:1–16

Hofstetter A, van Eck T, Shapira A (1996) Seismic activity along fault branches of the Dead Sea-Jordan transform system: the Carmel-Tirtza fault system. Tectonophysics 267:317–330

Hofstetter A, Klinger Y, Amrat A, Rivera L, Dorbath L (2007) Stress inversion and focal mechanisms along the Levantine Fault from seismological data. Tectonophysics 429:165–181

Hofstetter R, Gitterman Y, Pinsky V, Kraeva N, Feldman L (2008) Seismological observations of the Northern Dead Sea Basin earthquake on 11/2/2004. Isr J Earth Sci 57:101–124

Hofstetter A, Dorbath C, Calò M (2012) Crustal structure of the Dead Sea basin from local earthquake tomography. Geophys J Int 189:554–568

Kanamori H, Anderson D (1975) Theoretical basis of some empirical relations in seismology. Bull Seismol Soc Am 65:1073–1095

Le Beon M, Klinger Y, Amrat A-Q, Agnon A, Dorbath L, Baer G, Ruegg J-C, Charade O, Mayyas O (2008) Slip rate and locking depth from GPS profiles across the southern Dead Sea Transform. J Geophys Res 113. doi:10.1029/2007JB005280

Mayeda K, Malagnini L, Walter W (2007) A new spectral ratio method using narrow band coda envelopes: evidence for non-self-similarity in the Hector Mine sequence. Geophys Res Lett 14:11303–11308

Mechie J, Abu-Ayyash K, Ben-Avraham Z, El-Kelani R, Qabbani I, Weber M, DESIRE Group (2009) Crustal structure of the southern Dead Sea basin derived from project DESIRE wide-angle seismic data. Geophys J Int 178:457–478

Meirova T, Hofstetter A (2012) Observations of seismic activity in Southern Lebanon. J Seism. doi:10.1007/s10950-012-9343-2

Petrunin A, Meneses Rioseco E, Sobolev S, Weber M (2012) Thermomechanical model reconciles contradictory geophysical observations at the Dead Sea Basin. Geochem Geophys Geosyst 13:Q04011. doi:10.1029/2011GC003929

Rotstein Y, Bartov Y, Hofstetter A (1991) Active compressional tectonics in the Jericho area, Dead Sea Rift. Tectonophysics 198:239–259

Sadeh M, Hamiel Y, Ziv A, Bock Y, Fang P, Wdowinski S (2012) Crustal deformation along the Dead Sea Transform and the Carmel Fault inferred from 12 years of GPS measurements. J Geophys Res 117:B08410. doi:10.1029/2012JB009241

Salamon A (2005) Natural seismogenic effects of the 11 February 2004, M_L = 5.2, Dead Sea earth-quake. Isr J Earth Sci 54:145–169

Salamon A, Hofstetter A, Garfunkel Z, Ron H (1996) Seismicity of Eastern Mediterranean region: perspective of the Sinai subplate. Tectonophysics 263:293–307

Salamon A, Hofstetter A, Garfunkel Z, Ron H (2003) Seismotectonics of the Sinai Subplate – The Eastern Mediterranean Region. Geophys J Int 155:149–173

Shamir G, Eyal Y, Bruner I (2006) Localized versus distributed shear in transform plate boundary zones: the case of the Dead Sea transform in the Jericho Valley. Geochem Geophys Geosyst 6:1–21

Shapira A (1988) Magnitude scales for regional earthquakes monitored in Israel. Isr J Earth Sci 37:17–22

Shapira A (1997) On the seismicity of the Dead Sea basin. In: Niemi TM, Ben-Avraham Z, Gat JR (eds) The Dead Sea; the lake and its settings, Oxford monographs on geology and geophysics, no. 36. Oxford University Press, New York, pp 82–86

Shapira A, Feldman L (1987) Microseismicity of three locations along the Jordan rift. Tectonophysics 141:89–94

Shapira A, Hofstetter A (1993) Source parameters and scaling relationships of earthquakes in Israel. Tectonophysics 217:217–226

Shapira A, Hofstetter A (2002) Seismic parameters of seismogenic zones. Appendix C In: Shapira A 2002. An updated map of peak ground accelerations for Israel Building Code IS413, http://seis.gii.co.il/heb/hazards/docs/seismicity.pdf, Geophysical Institute of Israel Report 592/230/02, 74 p

Shapira A, Avni R, Nur A (1992) A new estimate for the epicenter of the Jericho earthquake of 11 July 1927. Isr J Earth Sci 42:93–96

ten Brink US, Ben−Avraham Z, Bell RE, Hassouneh M, Coleman DF, Andreasen G, Tibor G, Coakley B (1993) Structure of the Dead Sea pull−apart basin from gravity analysis. J Geophys Res 98:21877–21894

ten Brink US, Al-Zoubi AS, Flores CH, Rotstein Y, Qabbani I, Harder SH, Keller GR (2006) Seismic imaging of deep low-velocity zone beneath the Dead Sea basin and transform fault: implications for strain localization and crustal rigidity. Geophys Res Lett 33, L24314. doi:10.1029/2006GL027890

Thatcher W, Hanks T (1973) Source parameters of southern California earthquakes. J Geophys Res 78:8547–8576

Van Eck T, Hofstetter A (1989) Microearthquake activity in Dead Sea region. Geophys J Int 99:605–620

Van Eck T, Hofstetter A (1990) Fault geometry and spatial clustering of microearthquakes along the Dead Sea-Jordan fault zone. Tectonophysics 180:15–27

Wdowinski S, Bock Y, Baer G, Prawirodirdjo L, Bechor N, Naaman S, Knafo R, Forrai Y, Melzer Y (2004) GPS measurements of current crustal movements along the Dead Sea Fault. J Geophys Res 109:B05403

Weber M, DESERT Group (2004) The crustal structure of the Dead Sea Transform. Geophys J Int 156:655–681. doi:10.1111/j.1365-246X.2004.02143.x

Weber M, DESIRE Group (2009a) Anatomy of the Dead Sea Transform from lithospheric to microscopic scale. Rev Geophys 47:RGR2002, 44 pp

Weber M, DESIRE Group (2009b) Results of geophysical studies across the Dead Sea Transform: the Arava/Araba Valley and the Dead Sea Basin. Isr J Earth Sci 58:147–162

Wessel P, Smith W (1991) Free software helps maps and display data. EOS Trans AGU 72:441

Wiechert D (1980) Estimation of the earthquake recurrence parameters for unequal observation periods for different magnitudes. Bull Seismol Soc Am 70:1337–1346

Zhang H, Thurber CH (2003) Double-difference tomography: the method and its application to the Hayward fault, California. Bull Seismol Soc Am 93:1875–1889